Polymerization of Olefins Through Heterogeneous Catalysis. XVII. Experimental Study and Model Interpretation of Some Aspects of Olefin Polymerization Over a $TiCl_4/MgCl_2$ Catalyst

G. C. HAN-ADEBEKUN,* W. H. RAY

Department of Chemical Engineering, University of Wisconsin, 1415 Johnson Drive, Madison, Wisconsin 53706

Received 19 August 1996; accepted 6 September 1996

ABSTRACT: Using a high-activity $MgCl_2$-supported $TiCl_4$ catalyst, kinetic studies of ethylene and propylene polymerization are conducted in a semi-batch gas phase stirred-bed reactor system. Based on the experimental observations obtained from this study and others in the literature, simple kinetic mechanisms are proposed to explain the data. This model considers both the site formation from the interaction of catalyst and cocatalyst as well as the participation of monomers during site activation. By using this model together with parameters estimated from various sources, some aspects of kinetic behavior have been successfully predicted. These include the rate enhancement introduced by α-olefins, the effect of the Al/Ti ratio on kinetic features such as catalyst activity and decay rate, as well as the different reaction orders observed for various monomers. © 1997 John Wiley & Sons, Inc. J Appl Polym Sci **65:** 1037–1052, 1997

Key words: kinetics; Ziegler-Natta; olefin polymerization; gas phase

INTRODUCTION

Since the discovery of high-activity-supported titanium catalysts, intensive research efforts have been directed toward a comprehensive understanding of their structure and kinetic behavior.[1–3] In spite of their successful applications in industrial practice, a complete knowledge of these catalyst systems is still lacking. Some of the unresolved issues relate to the active site structure and its formation, as well as the role of components such as the cocatalyst and electron donor and their influence on the catalyst kinetic behavior.

Previous research seems to suggest two major functions of aluminum alkyl in olefin polymerization with transition metal catalysts; it acts as a key agent for transition metal oxidation state reduction, and also as an aid in bimetallic active site formation. Its role in the transition metal oxidation state reduction has been widely demonstrated through both physical analysis and chemical measurements. Using techniques such as electron spin resonance spectrometry (ESR),[4] photometry,[5] chemical ionization–mass spectrometry (CI-MS),[6] X-ray absorption spectroscopy,[7] and chemical titration methods,[5,8] the occurrence of oxidation state reduction upon the mixing of catalyst and cocatalyst has been confirmed. However, an explanation of the role of the aluminum alkyl in the active site structure is far from complete. This is especially true for the supported catalyst systems, where many more reactions could be possible due to additional components such as active supports and Lewis bases.

Even so, in the process of seeking the connection between the oxidation states and kinetic behaviour of these catalysts during polymerization,

Correspondence to: W. H. Ray.
* Present address: Eastman Kodak Co., Rochester, NY 14650-3059.
 CCC 0021-8995/97/061037-16

their sensitivity toward monomer type was examined. Studies begun by Soga, Ohnishi, and Sano[9] and continued by Kashiwa and Yoshitake[10] showed that Ti^{3+} is active for both ethylene and α-olefins, while Ti^{2+} is only active for ethylene. This seems to suggest that relating the different oxidation states to the active centers is a reasonable approach in model interpretation.

Studies also appear to indicate that the monomer plays a significant role in site activation. α-Olefins differ inherently from ethylene in several ways, including their considerable double bond polarity, high dipole moments,[11] and Lewis base nature.[12] Consequently, it is not surprising to observe that under the same operating conditions, ethylene polymerization exhibits kinetic behavior significantly different from that of other olefins. More generally, ethylene polymerization sites are much more stable than those of propylene, as has been observed in several studies.[13–21] Furthermore, the rate of propylene homopolymerization shows a linear dependence on monomer concentration,[15,22] while in ethylene polymerization, several reports have confirmed the existence of reaction orders higher than one.[22–24]

The fact that the phenomena noted above have not been quantitatively modeled or used to interpret other observed kinetic behavior provides the motivation for this article. Our objective was twofold. First, using a supported titanium catalyst of commercial importance, we conducted a series of experimental studies in a semi-batch gas phase reactor system in order to examine the roles of both the aluminum alkyl and different monomers during polymerization. These data were subsequently employed to postulate both a kinetic scheme and mathematical model in which the model parameters corresponding to the postulated mechanism were estimated. Secondly, the resulting kinetic models have been used to provide an interpretation of our results as well as those of other researchers. During the model development, a conscious attempt was made to limit the number of parameters. This greatly reduces the number of experiments required for parameter estimation, but it still yields a simple but realistic model suitable for predicting the observed kinetic behavior.

EXPERIMENTAL DESIGN

In this section, the experimental reactor system and procedures are described. A discussion of the postreaction analysis is also included.

Experimental System

Gas phase kinetic studies were performed in a one-liter stainless steel reactor (Parr Instrument Company). A detailed description of this experimental apparatus is presented in ref. 25.

In order to control the contact time of cocatalyst and catalyst, the catalyst injection device is designed to have three sections; the bottom section consists of the dry catalyst chamber while the mid-section contains the cocatalyst chamber. The top section contains the heptane bomb, which is used for washing the catalyst residue after the nitrogen injection. Swagelok ball valves connect the three sections so that an aging time varying from five minutes to several hours can be realized.

Experimental Procedures

In a typical polymerization run, the reactor is prepared by heat evacuation at $\sim$ 80°C for 2 h. A constant nitrogen purge is then applied at the same temperature for an hour and the reactor is brought to the reaction temperature. Simultaneously, catalyst and cocatalyst are loaded into the corresponding chambers of the catalyst injection device (previously stored under vacuum at 40–45°C for at least 2 h). Catalyst aging is initiated by opening the valves connecting the catalyst and cocatalyst chambers. They remain contacted at room temperature for the required period of time. Following this, the mixture of catalyst and cocatalyst is injected into the reactor by means of nitrogen overpressure. The catalyst injection process is completed by several heptane washes and nitrogen shots; polymerization is then initiated by the introduction of monomer.

Postreaction Analysis

The postreaction analysis carried out includes a comparison among the following methods: integrated yield, gravimetric yield (Fig. 1), and residual metal analysis of polymer. Analysis of the residual metals (Ti, Mg, and Al) in the polymer was used as a consistency check for the effectiveness of the catalyst and cocatalyst delivery system.[26] For residual metal, neutron activation analysis (NAA)[27] was employed. This nondestructive technique has several advantages over other methods which are in common usage.[28] Titanium content and Al/Ti ratio obtained from the NAA measurements were compared with those calculated from

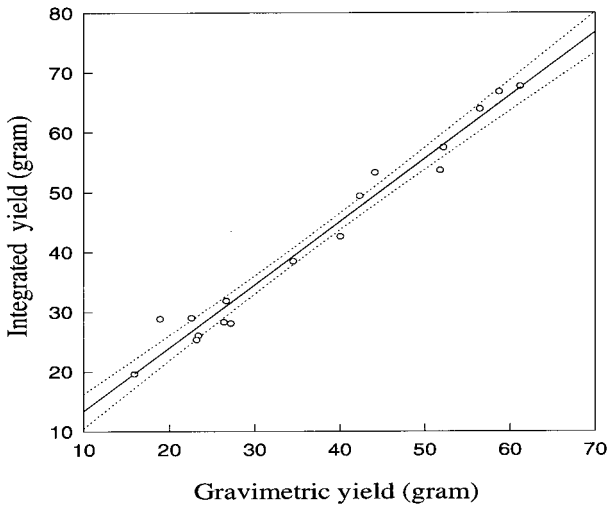

Figure 1 Comparison between the integrated yield and gravimetric yield obtained in the gas phase reactor system. The dashed lines represent the 95% confidence interval.

the catalyst and cocatalyst loadings and showed that consistent delivery of catalyst and cocatalyst was achieved within the experimental region. As a further check, the magnesium content in the final polymer, which comes from the support, was found to increase linearly with titanium content.

EXPERIMENTAL OBSERVATIONS

All the experiments presented below were conducted at 50 ± 1°C using a high-activity magnesium chloride-supported titanium catalyst. Triethyl aluminum (TEA) was used as the cocatalyst in all the studies.

To study the possible participation of monomer in site activation, the instantaneous reaction rates of ethylene and propylene are compared. Their responses as a function of the monomer concentration are also investigated. To examine the role of TEA in site formation, the effect of the Al/Ti ratio on ethylene homopolymerization is examined. Finally, the effect of catalyst aging time on both ethylene and propylene homopolymerization is studied.

Instantaneous Reaction Rate Curves

In general, ethylene exhibits reaction rate curves quite different from those of propylene (Fig. 2). While the propylene homopolymerization rate decreases continuously, the ethylene rate reaches a stationary activity (which decreases very slowly, if at all).

An examination of the effect of intermittent removal and re-introduction of monomer on the reaction rate curve indicates that both ethylene and propylene rates return quite close to their characteristic rates after the perturbation. This suggests that in both cases a diffusion limitation is not responsible for the observed deactivation. However, the restored reaction rate curve after the interruption and subsequent re-introduction reveals that an activation period of ~ 30 min is required for ethylene polymerization to reach its final rate, while none exists for propylene polymerization.

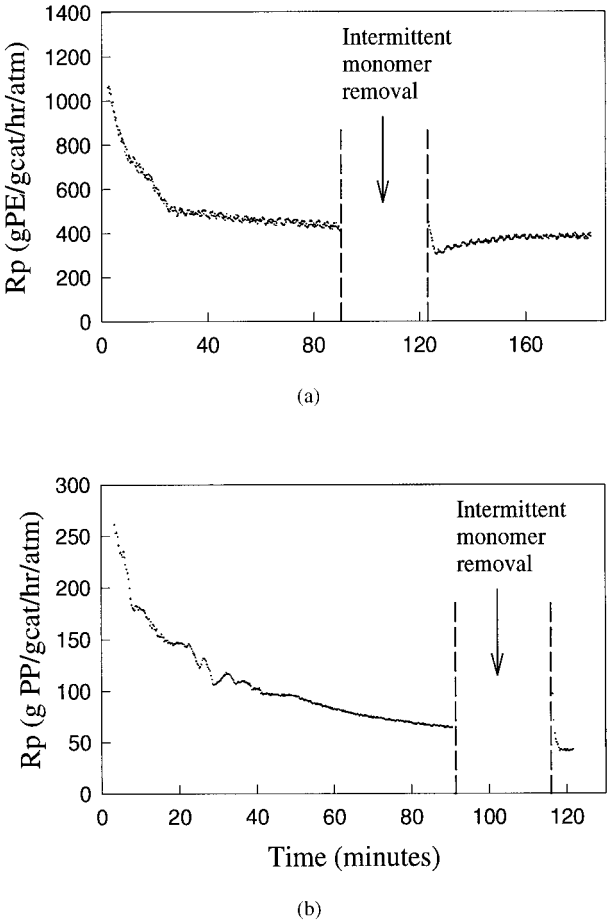

Figure 2 Polymerization reaction rate as a function of reaction time. (a) Ethylene homopolymerization; (b) propylene homopolymerization. (T = 50°C, Al/Ti = 85.5, P_{C_2} = 2.4 atm, P_{C_3} = 3 atm).

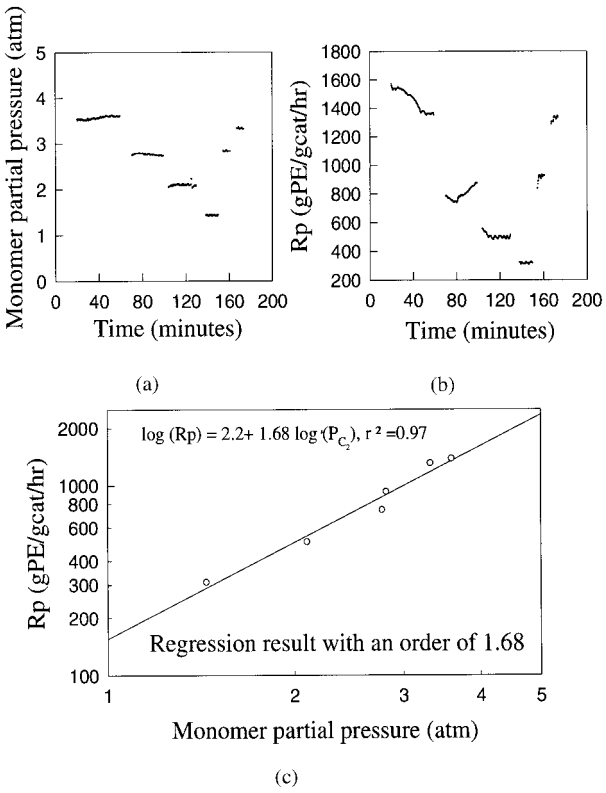

Figure 3 Influence of ethylene partial pressure on polymerization reaction rates. (a) Monomer partial pressure sequence; (b) the resultant change in reaction rate; (c) log–log plot of reaction rate versus ethylene pressure. (T = 50°C, Al/Ti = 86.5).

Effect of Monomer Concentration

The effect of monomer concentration (partial pressure) on the olefin homopolymerization rate is investigated during a single reaction run. This is a good example illustrating the advantages of employing a gas phase reactor system for the kinetic studies. The absence of liquid phase mass transfer resistance and the rapid equilibrium of gas species with the polymer means that the system is easy to change from one operating condition to another.

For ethylene polymerization, Figure 3 shows the resultant changes in reaction rate (plot b) when the monomer partial pressure change sequence (plot a) is impressed on the system. A plot of the plateau reaction rate versus monomer partial pressure (plot c) shows a reaction order of 1.68. It may be observed that this effect is completely reversible.

By contrast, for propylene homopolymerization, the same experiment produces a reaction order close to 1 (Fig. 4). This is consistent with the results in other studies[22,29] over the typical monomer concentration range. However, because of the much stronger catalyst decay for propylene polymerization, the reversible nature is difficult to observe.

Effect of Al/Ti Ratio

In the literature it is known that the effect of Al/Ti on propylene polymerization rate shows a maximum activity at a certain optimum Al/Ti ratio ($\approx$ 15). This is reported for both slurry phase systems[14,15] and gas phase reactor systems.[30]

Consequently, an experimental study focusing only on ethylene homopolymerization with different Al/Ti ratios was conducted. A reaction temperature of 50°C and a catalyst aging time of $\sim$ 25 min were employed. For ethylene homopolymerization, both an optimum activity behavior (with optimal Al/Ti ratios of 60[31] to 100[32]) as well as a

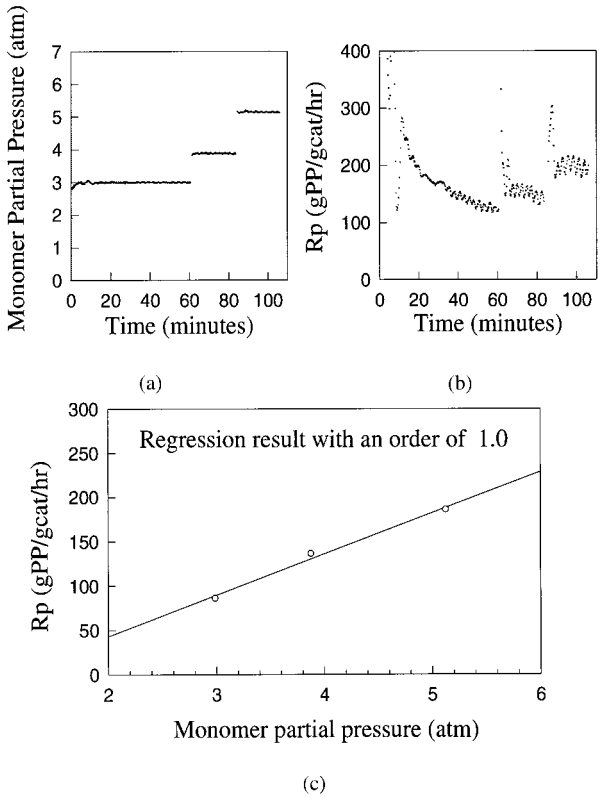

Figure 4 Influence of propylene partial pressure on polymerization reaction rates. (a) Monomer partial pressure sequence; (b) the resultant change in reaction rate; (c) reaction rate versus propylene pressure plot (T = 50°C, Al/Ti = 86.5).

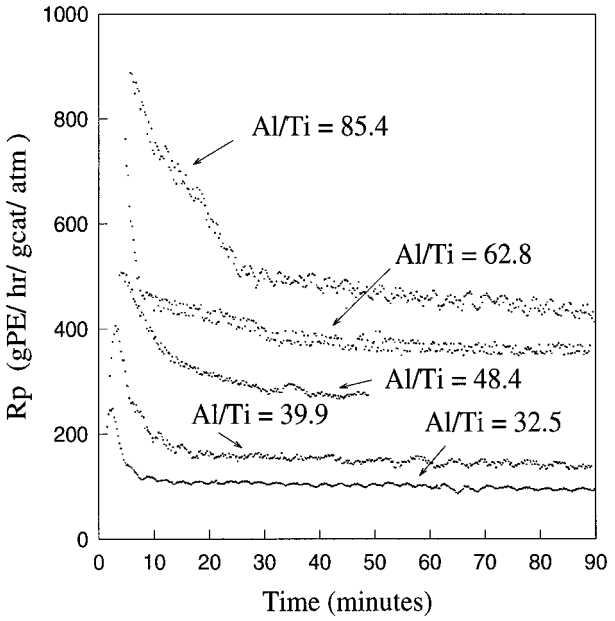

Figure 5 Effect of Al/Ti ratios on ethylene homopolymerization reaction rates. (T = 50°C, catalyst aging time = 25 min, $P_{C_2} \approx 2$ atm).

monotonic increase of activity (with Al/Ti in the range of 10 to 120)[2] have been previously observed. Although the monotonic increase might be the increasing part of the overall optimum curve, it is in general true that ethylene polymerization has a much higher optimum Al/Ti ratio compared with that of propylene. The results shown in Figure 5 bear a resemblance to those in other published work.[2]

Effect of Catalyst Aging

Using the catalyst injection device described previously, the influence of catalyst aging on reaction rates has been examined. From Figure 6, it is seen that both the ethylene and propylene reaction rate curves follow the unperturbed master curve after the initiation of the monomer feed. These same phenomena have been reported by Pino and Rotzinger[19] in the slurry phase reactor for both ethylene and propylene, as well as by Keii et al.[18] and Chien, Weber, and Hu[8] for slurry propylene polymerization. These studies indicate that the catalyst activity is strongly influenced by the action of the cocatalyst whether or not polymerization is taking place.

MODEL DEVELOPMENT

Based on the experimental observations, a realistic model must account for both the role of TEA in site formation as well as monomer participation in site activation. This is accomplished in two separate steps. First, we focus on the potential site (C_{pot}) formation through the reaction of catalyst and cocatalyst. Subsequently, we allow C_{pot} to be activated by monomer to form an active site (P^{act}).

Site Formation from Catalyst and Cocatalyst Interaction

In this section, a model is proposed for the catalyst/cocatalyst interaction and the parameters of the model are estimated. When $TiCl_4$ catalyst and

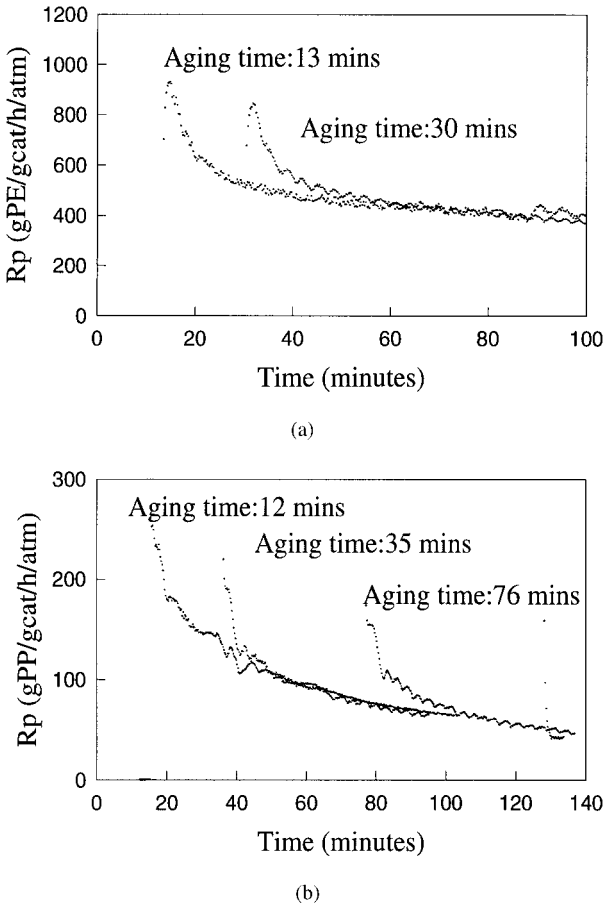

Figure 6 Influence of aging time on the polymerization reaction rate. (a) Ethylene homopolymerization; (b) propylene homopolymerization (T = 50°C, Al/Ti = 85.1 ± 0.5, P_{C_2} = 1.7 atm, P_{C_3} = 3.0 atm).

aluminum alkyl are mixed, a series of chemical reactions take place,[33] which can result in changes in the oxidation state of the transition metal (Ti).

Experimental investigations of catalyst/cocatalyst reactions can be traced back to the late 1950s when quantitative studies of the reaction kinetics were carried out by various researchers.[34–36] It was then experimentally observed that when $TiCl_4$ is mixed with alkylaluminum compound, the first reaction step consists of a ligand exchange, which proceeds rapidly.[37] This is then followed by the reductive dealkylation to a lower valence state which is believed to be the rate-determining step. A similar mechanism may be assumed to account for further reductions to even lower valence states. The degree of reduction depends on the Al/Ti ratio employed, the contact time, and the temperature at which the catalyst/cocatalyst contact occurs. The assumed mechanism is given by the following steps:

$$\mathrm{TiCl_4} + \mathrm{AlEt_3} \overset{ka_1, ka_{-1}}{\rightleftharpoons} \mathrm{EtTiCl_3} + \mathrm{AlClEt_2}$$

$$\mathrm{EtTiCl_3} \overset{kad_1}{\rightarrow} \mathrm{TiCl_3} + \mathrm{Et}. \qquad (1)$$

For supported catalyst with various components present, the reactions are believed to be quite complicated.[4,38] Although it appears that besides acting as a reducing agent, TEA also participates in the active site formation through the formation of bimetallic active centers,[18,39] the true nature of the structure and mechanism is still uncertain.[29] Therefore, a simple schematic model is adopted here. It is based on the stepwise titanium oxidation state evolution mechanism which is well accepted[10] as described in eq. (2).

$$\mathrm{Ti^{4+}} + \mathrm{AlEt_3} \overset{kad_1}{\rightarrow} \mathrm{Ti^{3+}} + (\text{byproducts})$$

$$\mathrm{Ti^{3+}} + \mathrm{AlEt_3} \overset{kad_2}{\rightarrow} \mathrm{Ti^{2+}} + (\text{byproducts})$$

$$\mathrm{Ti^{2+}} + \mathrm{AlEt_3} \overset{kad_3}{\rightarrow} \mathrm{Ti^{+}} + (\text{byproducts}) \qquad (2)$$

The differential equations describing the dynamic change of oxidation states can be derived from this kinetic mechanism as

$$\frac{d[\mathrm{Ti^{4+}}]}{dt} = -kad_1[\mathrm{TEA}][\mathrm{Ti^{4+}}]$$

$$\frac{d[\mathrm{Ti^{3+}}]}{dt} = kad_1[\mathrm{TEA}][\mathrm{Ti^{4+}}] - kad_2[\mathrm{TEA}][\mathrm{Ti^{3+}}]$$

$$\frac{d[\mathrm{Ti^{2+}}]}{dt} = kad_2[\mathrm{TEA}][\mathrm{Ti^{3+}}] - kad_3[\mathrm{TEA}][\mathrm{Ti^{2+}}]$$

$$\frac{d[\mathrm{TEA}]}{dt} = -(kad_1[\mathrm{Ti^{4+}}] + kad_2[\mathrm{Ti^{3+}}] + kad_3[\mathrm{Ti^{2+}}])[\mathrm{TEA}] \qquad (3)$$

with initial values:

$$[\mathrm{Ti^{4+}}](t = 0) = [\mathrm{Ti^{4+}}]_o$$

$$[\mathrm{Ti^{3+}}](t = 0) = [\mathrm{Ti^{3+}}]_o$$

$$[\mathrm{Ti^{2+}}](t = 0) = [\mathrm{Ti^{2+}}]_o$$

$$[\mathrm{TEA}](t = 0) = \left(\frac{\mathrm{Al}}{\mathrm{Ti}}\right)_{\mathrm{eff}}$$

where $[\mathrm{Ti^{N+}}]\left([=]\frac{\mathrm{mol}}{\mathrm{mol\ Ti}}\right)$ is the mole fraction of total titanium of oxidation state N+, [TEA] $\left([=]\frac{\mathrm{mol\ Al}}{\mathrm{mol\ Ti}}\right)$ is concentration of TEA based on titanium, and $\left(\frac{\mathrm{Al}}{\mathrm{Ti}}\right)_{\mathrm{eff}}$ is the effective Al/Ti ratio present initially in the system. Because of the complex side reactions involved in supported catalysts, the experimental Al/Ti ratio is often much greater than the stoichiometric ratio. Therefore, when supported catalysts are under study, an effective Al/Ti ratio is used in the model to represent the "true" aluminum alkyl participating in the oxidation state reduction. As a result, $\left(\frac{\mathrm{Al}}{\mathrm{Ti}}\right)_{\mathrm{eff}}$ is an estimated model parameter.

In order to have a model suitable for simulation, the model parameters must be estimated step by step from different experimental sets. Parameter kad_1 is estimated based on data from Beermann and Bestian,[34] where pure chemical reaction of $TiCl_4$ and $AlEt_3$ was studied (Fig. 7). Parameter kad_2 is estimated from comprehensive data in Chien, Weber, and Hu,[8] where a supported $TiCl_4$ catalyst was under study (Fig. 8). During this process, to fit experimental Ti^{4+} data reported by Chien while using previously esti-

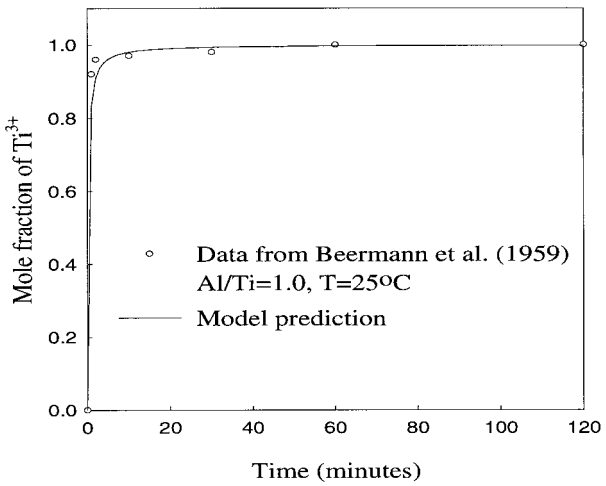

Figure 7 Evolution of titanium oxidation states as a function of aging time showing experimental data from Beermann and Bestian[34] (circles) and model predictions (lines).

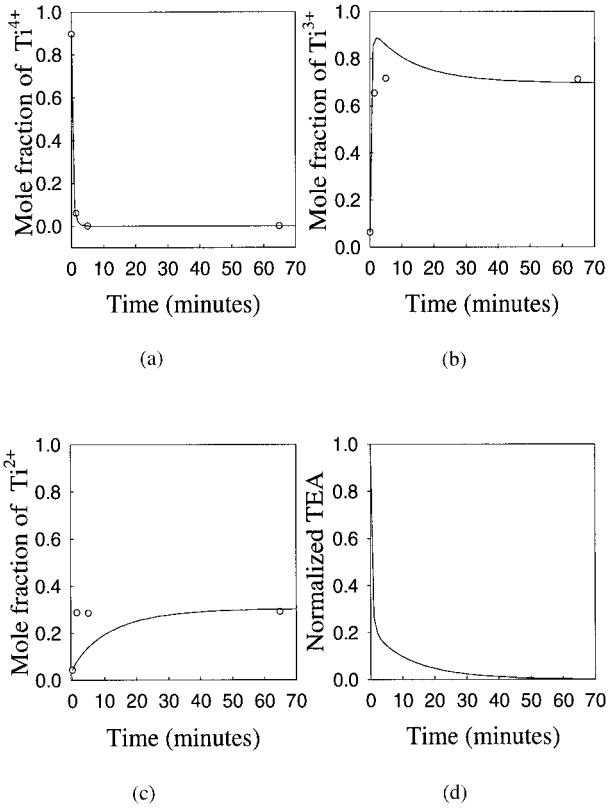

Figure 8 Evolution of titanium oxidation states as a function of aging time showing experimental data from Chien, Weber, and Hu[8] (circles) and model predictions (lines) with an effective Al/Ti = 1.16.

Table I Model Parameters for Site Formation

Parameters	Units	Estimated Values
kad_1 ($Ti^{4+} \rightarrow Ti^{3+}$)	$\frac{\text{mol Ti}}{\text{mol Al, min}}$	5.00
kad_2 ($Ti^{3+} \rightarrow Ti^{2+}$)	$\frac{\text{mol Ti}}{\text{mol Al, min}}$	9.30×10^{-2}
kad_3 ($Ti^{2+} \rightarrow Ti^{+}$)	$\frac{\text{mol Ti}}{\text{mol Al, min}}$	1.73×10^{-3}

mated kad_1 value, $\left(\frac{\text{Al}}{\text{Ti}}\right)_{\text{eff}}$ is estimated to be 1.16. kad_2 is then estimated through the fitting of experimental Ti^{3+} and Ti^{2+} data.[8] Finally, kad_3 is calculated assuming that $kad_1/kad_2 = kad_2/kad_3$.

In order to fit the flat Ti^{3+} and Ti^{2+} profile experimentally observed by Chien, Weber, and Hu,[8] (Fig. 8), the fast depletion of free cocatalyst is necessary. The estimated model parameters are shown in Table I; these estimates are maintained at the values in that table in all subsequent material.

Using the estimated model parameters, the average titanium oxidation state after 30 minutes of reaction is examined at various Al/Ti ratios. Figure 9 contains the model predictions together with experimental data by various investigators.[35,40,41]

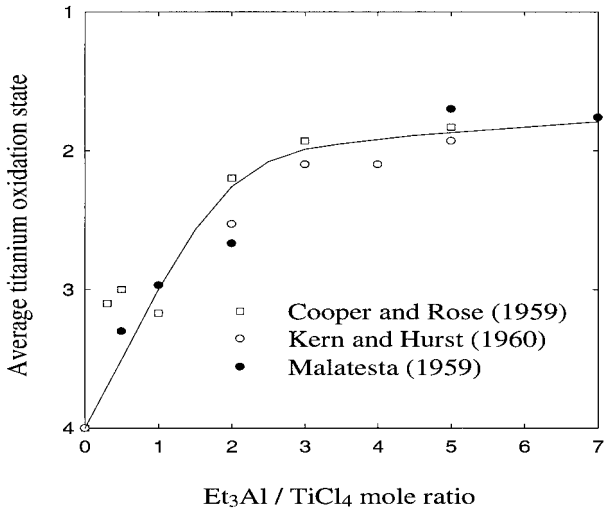

Figure 9 Average titanium oxidation state versus Al/Ti mole ratio after 30 min at 25°C showing experimental data from different authors (refs. 35, 40, 41) and model predictions (lines) using estimated parameters in Table I.

Participation of Monomers in Site Activation

Having modeled the formation of potential sites, C_{pot}, through the catalyst/cocatalyst reactions, we now describe the modeling approach taken in accounting for the role of monomers in site activation.

To explain the experimental observations discussed previously, a two-step propagation kinetic model which includes reversible site activation by monomer has been proposed by various investigators.[11,23,24] Mathematically, this is described by eq. (4).

$$C_{pot} + [M] \overset{k_f, k_b}{\rightleftharpoons} P^{act}$$

$$P_n^{act} + [M] \overset{k_p}{\rightarrow} P_{n+1}^{act} \qquad (4)$$

where C_{pot} represents the concentration of potential sites, P^{act} the concentration of total active sites, and P_n^{act} the concentration of live polymer chains with chain length of n ($P^{act} = \sum_{n=0} P_n^{act}$).

An analytical solution to this model for the catalyst particle yields an expression both for the dependence of P_n^{act} on monomer concentration as well as for the rate of approach to equilibrium as

$$P^{act} = \frac{K[M]C_\infty}{K[M] + 1}\{1 - e^{-k_b(K[M]+1)t}\}$$

$$R_p = k_p P^{act}[M] \qquad (5)$$

where K equals $\frac{k_f}{k_b}$ and C_∞ is the total concentration of active sites. Using this model, a variable order dependence of reaction rate on monomer concentration can be obtained as is shown below.

Case 1: $K[M] \gg 1$

In this case, a first order dependence of rate on monomer concentration arises and the speed of site formation is mainly determined by the forward rate constant k_f. This is clearly the case for α-olefins. For certain monomer concentration values, selecting $\frac{k_f}{k_b}$ sufficiently large ensures this condition. For typical operating conditions under this study, monomer partial pressures are in the range of 1–5 atm and reaction temperatures are in the range of 50–80°C. Using the sorption factor as defined in Hutchinson and Ray,[42] monomer concentrations $[M]$ can be calculated to be on the order of 0.1–0.5 $\frac{\text{moles}}{L \text{ amorphous polymer}}$. Accordingly, in the subsequent material, $\frac{k_f}{k_b}$ is taken to be 208.3.

Case 2: $K[M] < 1$

Here, a reaction order higher than one results and k_b determines the site formation rate. The polymerization of ethylene clearly belongs to this regime. For the same operating conditions as in Case 1, selecting reasonable values of $\frac{k_f}{k_b}$ ensures this condition. In this study, $\frac{k_f}{k_b}$ is taken to be 8.0.

Note that the success of the mathematical representation notwithstanding, the physical picture of this equilibrium step mechanism is still not precisely defined. However, this model is consistent with two proposed physical mechanisms: (1) the monomer insertion is triggered by a second monomer in the so-called "Triggering" model,[43] and (2) monomer occupies one of the two vacant sites and serves as a ligand. The ultimate kinetic behavior is a result of competitive equilibria among the unsaturated transition metal center, the aluminum alkyl, and various coordinating ligands.[23]

For both of these physical pictures, the model is based on the simple ideas presented earlier in eq. (4), but extended to include two monomers and two potential active sites. Thus, we have

$$C_{pot}^k + [M_j] \overset{k_{fj}^k, k_{bj}^k}{\rightleftharpoons} P^{act}{}_j^k$$

$$P_n^{act}{}_j^k + [M_i] \overset{k_{pji}^k}{\rightarrow} P_{n+1}^{act}{}_j^k \qquad (6)$$

The physical representation of site i is based on the transition metal oxidation states as described previously: site 1 is directly related to Ti^{3+}, while site 2 is related to Ti^{2+}. Since the transformation from Ti^{4+} to Ti^{3+} is usually complete within the catalyst/cocatalyst precontacting period, its contribution to the chain growth is not considered. Then the total number of sites in each oxidation state is given by

$$[Ti^{3+}]F_{\text{active site}} = C_{pot}^1 + \sum_{j=1}^{Nm} P^{act}{}_j^1$$

$$[Ti^{2+}]F_{\text{active site}} = C_{pot}^2 + \sum_{j=1}^{Nm} P^{act}{}_j^2 \qquad (7)$$

where $P_n^{\text{act}\,k}{}_j$ represents the concentration of total active sites of type k, which is activated by monomer j and $P_n^{\text{act}\,k}{}_j$ is the concentration of live polymer chains with chain length of n, and $F_{\text{active site}}$ is the molar fraction of active transition metal. The following relationships exists between $P_n^{\text{act}\,k}{}_j$ and $P^{\text{act}\,k}{}_j$:

$$P^{\text{act}\,k}{}_j = \sum_{n=0}^{\infty} P_n^{\text{act}\,k}{}_j \tag{8}$$

For both Ti^{3+} and Ti^{2+} sites, an overall first-order spontaneous deactivation (k_{spd}) is assumed. This is based on the experimental observation from Chien, Weber, and Hu,[8] where even under a constant oxidation state distribution, an obvious deactivation still exists for propylene polymerization.

The mathematical equations describing this kinetic mechanism are given by

$$\begin{aligned}\frac{dP^{\text{act}\,k}{}_j}{dt} &= k_f{}^k{}_j[M_j]C^k_{\text{pot}} - k_b{}^k{}_j P^{\text{act}\,k}{}_j \\ &\quad - kad_2 P^{\text{act}\,1}{}_j[\text{TEA}]\delta(k-1) \\ &\quad + (kad_2 P^{\text{act}\,1}{}_j - kad_3 P^{\text{act}\,2}{}_j)[\text{TEA}] \\ &\quad \times \delta(k-2) - k^k_{spd} P^{\text{act}\,k}{}_j \end{aligned} \tag{9}$$

Monomer consumption rates:

$$R_p^k(M_i) = \sum_{j=1}^{N_m} k_p{}^k{}_{ji} F_{\text{active site}} P^{\text{act}\,k}{}_j[M_i]$$

where $k_p{}^k{}_{ji}$ is the chain propagation rate constant in the unit of $\dfrac{L \text{ amorphous polymer}}{\text{mol, mol active site, min}}$ and $R_p^k(M_i)$ is the consumption rate of monomer i in the unit of $\dfrac{\text{mol}}{\text{mol transition metal, min}}$.

Table II shows the set of parameters fitted to the experimental data obtained for ethylene and propylene homopolymerization under identical operating conditions (Fig. 10). It is obvious that for ethylene homopolymerization, the simple model has difficulty in predicting the initial decaying reaction rate. Further work is needed to understand this.

The dependence of reaction rate on the monomer concentrations is plotted in Figure 11. They match the experimental observations quite well, with an order of 1.66 for ethylene and 1.02 for propylene.

EXAMPLES

With the model equations established and the model parameters listed, some other results observed in previous experimental work by various researchers are simulated. This is done with a view to evaluating the ability of our model to predict these observations. Thus, we consider the possible contribution of oxidation state reduction to site deactivation (example 1), the effect of Al/Ti ratio on ethylene and propylene homopolymerization (example 2), the enhancement effect on ethylene polymerization rate due to the addition of 1-hexene (example 3), and the change in reaction order with ethylene pressure when 1-hexene is present (example 4).

Example 1: Role of Oxidation State Reduction in Deactivation

Let us use the model to interpret some slurry polymerization results from Keii et al.[18] They examined the effect of elimination of TEA during polymerization on the observed decay rate. After an interruption in polymerization, the residual solids were washed with heptane to remove TEA; the subsequent polymerization rate with the washed solids in the absence of TEA was observed to be lower and its decay rate slower when compared with that of the unperturbed case. Once the TEA was reintroduced into the system, both the polymerization rate and the decay rate returned to the original values (Fig. 12).

This experiment strongly suggests the possible role of oxidation state reduction in the site deactivation. In order to illustrate this in more detail, a simulation is carried out using the proposed model. First, the model parameters (Table III) are obtained by fitting the propylene homopolymerization rate under the normal operating condition (the unperturbed reaction rate curve shown in Fig. 12). Subsequently, the effect of elimination and re-admission of TEA is simulated as a change in the effective Al/Ti during the reaction and the influences both on oxidation state and on site activation.

As is shown in Figure 13, the change in the decay rate is clearly demonstrated both during the low TEA period as well as after the re-intro-

Table II Model Parameters for Ethylene and Propylene Polymerization (50°C, Al/Ti = 86.5)

Parameters	Units	Estimated Values
Potential Site-Related		
Effective Al/Ti	(—)	1.9
kspd	min^{-1}	2.0×10^{-3}
Propylene Polymerization		
$k_f(Ti^{3+})$	$\frac{L \text{ amorphous polymer}}{\text{mol, min}}$	5.0
C_3 propagation $k_p(Ti^{3+})$	$\frac{L \text{ amorphous polymer}}{\text{mol, mol transition metal, min}}$	3.8×10^3
Ethylene Polymerization		
$k_f(Ti^{3+}, Ti^{2+})$	$\frac{L \text{ amorphous polymer}}{\text{mol, min}}$	8.0×10^{-1}
C_2 propagation $k_p(Ti^{3+})$	$\frac{L \text{ amorphous polymer}}{\text{mol, mol transition metal, min}}$	6.0×10^4
$\frac{k_p(Ti^{2+})}{k_p(Ti^{3+})}$	(—)	1.3

Note: $k_p\left[\frac{L \text{ amorphous polymer}}{\text{mol, mol transition metal, min}}\right] = k_p\left[\frac{L \text{ amorphous polymer}}{\text{mol, mol active site, min}}\right] F_{\text{active site}}$

duction of TEA. For added comparison, the change in Ti^{3+} during the entire process is also plotted, indicating that the change in decay rate may be due to the slowdown in the reduction of Ti^{3+} to Ti^{2+}.

Example 2: Effect of Al/Ti on Catalyst Activity

As was previously stated, when the effect of Al/Ti on propylene polymerization was studied, a maximum activity was observed at an optimum Al/Ti ratio ranging from 20 to 60. However, when decay rate was investigated as a function of Al/Ti ratio, it was reported that propylene deactivation shows a transition from first-order decay at a low Al/Ti level to second-order decay at a higher Al/Ti ratio.[15,44] A possible explanation for this lies in the fact that the oxidation state distribution can change at different levels of Al/Ti. This is simulated using the proposed model with parameters from Table II.

As is shown in Figure 14, when the effective Al/Ti ratio is changed from 0.5 to 1.9, the propylene polymerization rate shows an initial increase followed by a decrease, with the deactivation becoming more severe at higher Al/Ti ratios. From the change of Ti^{3+} shown in the figure, the initial increase is due to more Ti^{3+} production at the expense of Ti^{4+}. When more TEA is added into the system, all the Ti^{4+} is transformed to Ti^{3+}, and over-reduction becomes dominant.

The situation is, however, quite different for ethylene polymerization, where both Ti^{3+} and Ti^{2+} are active for the polymerization reaction. Note that as is shown in Figure 15, the increase in catalyst activity could level off at a very high Al/Ti ratio when all the Ti^{3+} has been reduced to Ti^{2+}. If the Al/Ti ratio continues to increase, a rate decrease similar to those observed from propylene polymerization can be obtained. However, in this case, it is due to the over-reduction of Ti^{2+} to Ti^{+}; the latter is not active for polymerization.

Example 3: Ethylene Copolymerization with 1-Hexene

In order to study the cause of rate enhancement in ethylene/α-olefin copolymerization, a detailed experimental study was carried out by Calabro and Lo[45] for ethylene copolymerization with 1-hexene. These researchers observed that the rate enhancement effect is sensitive to the point (in time) of hexene addition relative to the initiation of polymerization. If hexene is present initially, the effect is most pronounced. Furthermore, delaying the hexene injection to an ongoing ethylene polymerization alters the observed kinetics only

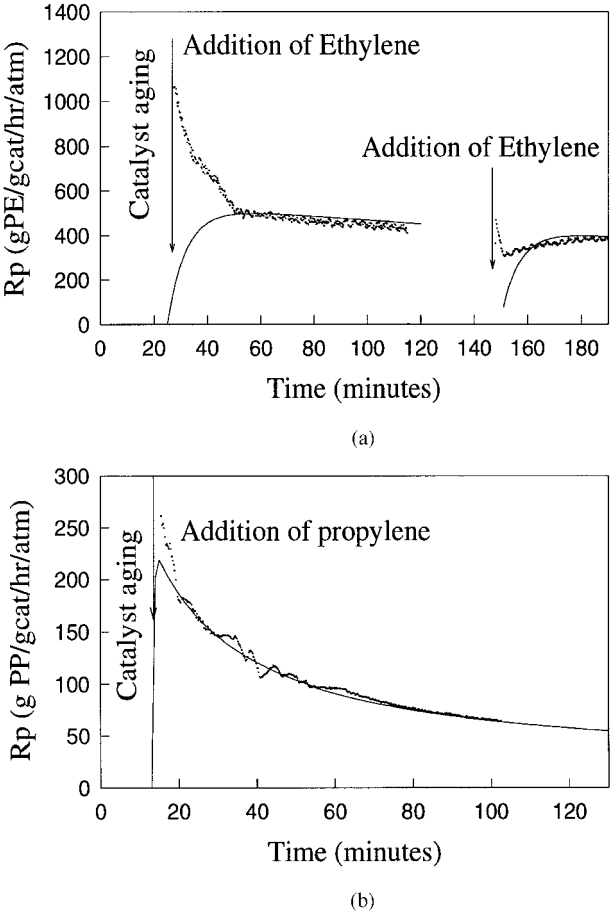

Figure 10 Polymerization reaction rates as a function of reaction time for a stirred bed gas phase reactor system; the solid lines represent the model simulation, the dotted lines represent the experimental observations. (a) Ethylene homopolymerization; (b) propylene homopolymerization (T = 50°C, Al/Ti = 85.5, P_{C_2} = 2.4 atm, P_{C_3} = 3 atm).

if it occurs before the reaction attains maximum activity. This is shown in Figure 16.

Using our proposed model, the experimentally observed ethylene homopolymerization and copolymerization rates are fitted in order to obtain the model parameters (Table IV).

Figure 17 shows the comparison between the experimental data and the model prediction, while Figure 18 shows the diminishing rate enhancement effect simulated by the model; note that Figure 18 predicts similar results as those obtained experimentally (Fig. 16).

To further demonstrate the plausibility of our

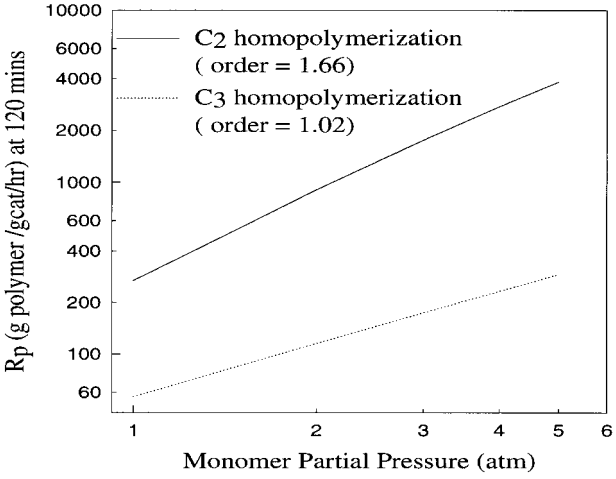

Figure 11 Model simulation: the dependence of ethylene and propylene homopolymerization rates on monomer concentrations. The simulated reaction conditions are the same as those in Figure 10.

results, in Figure 19, the concentrations of Ti^{3+}-type sites activated by the two monomers are presented. Since 1-hexene is much faster than ethylene in activating the potential sites, when 1-hexene is introduced simultaneously with ethylene, all the available potential sites can be activated immediately. If hexene is added after

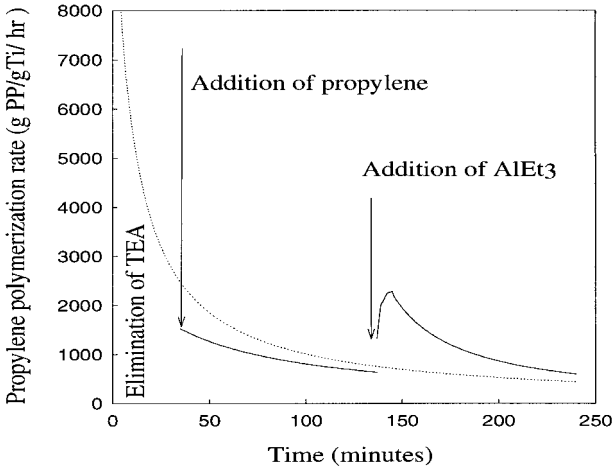

Figure 12 Elimination of solute TEA during the propylene polymerization; the dashed line represent the kinetic curve for the unperturbed polymerization; the solid lines represent those obtained after the elimination and re-introduction of TEA during the reaction (experimental data from Keii et al.[18]).

Table III Model Parameters for Propylene Polymerization Estimated from Data by Keii et al.[18]

Parameters	Units	Estimated Values
Effective Al/Ti	(—)	0.9
kspd	min^{-1}	6.0×10^{-3}
Propylene Polymerization		
$k_f(Ti^{3+})$	$\frac{L \text{ amorphous polymer}}{\text{mol, min}}$	5.0
C_3 propagation $k_p(Ti^{3+})$	$\frac{L \text{ amorphous polymer}}{\text{mol, mol transition metal, min}}$	2.4×10^3

ethylene has had the chance to participate in site activation, the number of available potential sites decreases. As seen in the figure [plots (a) and (b)], if the addition of hexene is delayed after the sites are fully activated by ethylene, hexene loses its chance in the competition, resulting in the fact that hexene has little effect on the reaction rate. This effect is further en-

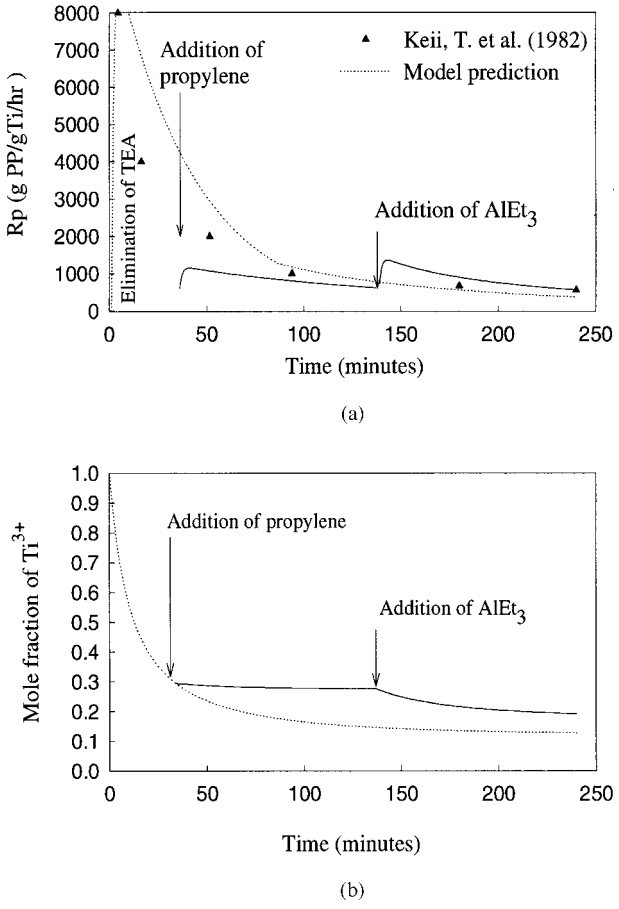

Figure 13 Model simulation examining the effect of TEA on catalyst deactivation during propylene polymerization; the dashed lines represent the kinetic curve for unperturbed polymerization; the solid lines represent those obtained after the elimination and re-introduction of TEA; triangles are experimental data from Keii et al.[18] (a) Reaction rate versus reaction time; (b) evolution of Ti^{3+} during the reaction.

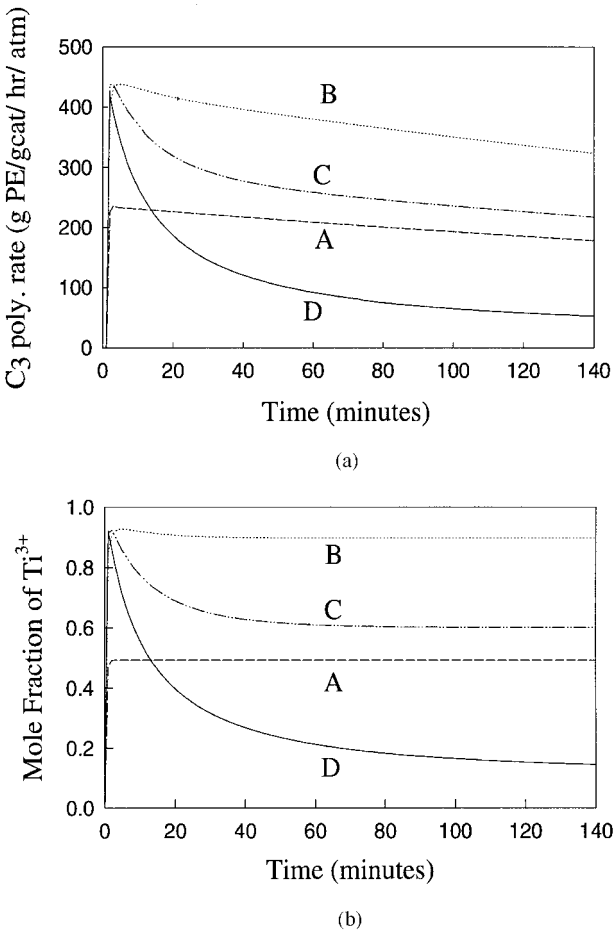

Figure 14 Effect of Al/Ti ratio on propylene homopolymerization rates; effective Al/Ti ratio of 0.5 (A), 1.1 (B), 1.4 (C), and 1.9 (D). (a) Reaction rate versus reaction time; (b) change of Ti^{3+} during the reaction.

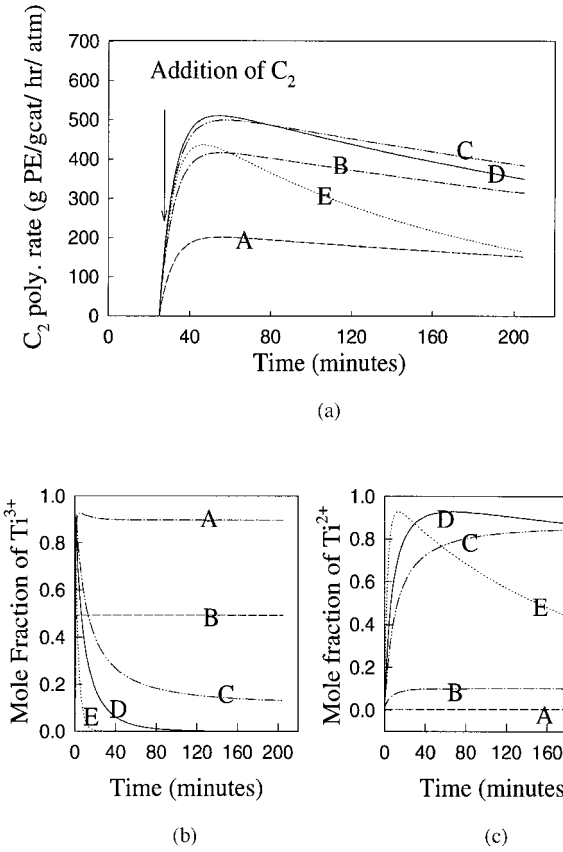

Figure 15 Effect of Al/Ti ratio on ethylene homopolymerization rate; effective Al/Ti ratio of 0.5 (A), 1.1 (B), 1.9 (C), 2.5 (D), and 5.0 (E). (a) Reaction rate versus time; (b) change of Ti^{3+} during the reaction; (c) change of Ti^{2+} during the reaction.

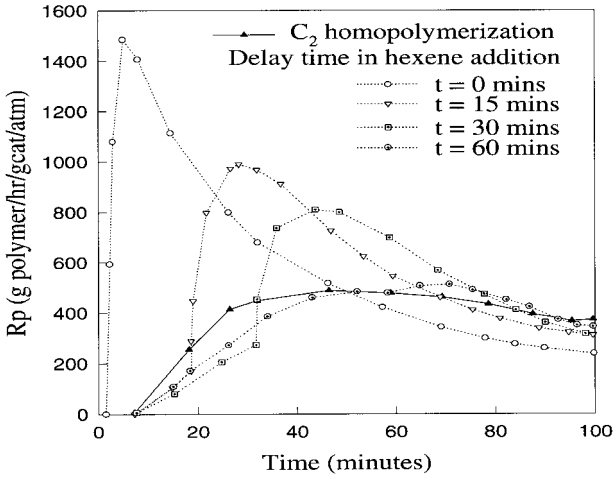

Figure 16 Experimental data examining the effect of hexene addition on reaction kinetics of ethylene homopolymerization (ref. 45) ($RMgX/TiCl_4$/TEA catalyst, T = 80°C, Al/Ti = 80, C_6/C_2 = 2.08, P_{C_2} = 4.8 atm).

hanced by the continuous reduction of Ti^{3+} to Ti^{2+}; the latter site may not be activated by 1-hexene.

Example 4: Reduction of Monomer Reaction Order in the Presence of 1-Hexene

Using a stannic chloride modified $TiCl_4/MgCl_2$ catalyst system, Kryzhanovskii, Gapon, and Ivan-

Table IV Model Parameters for Ethylene/1-Hexane Polymerization Estimated from Data by Calabro and Lo[45]

Parameters	Units	Estimated Values
Effective Al/Ti	(—)	1.2
kspd	min^{-1}	1.8×10^{-2}
Site Activated by Ethylene		
$k_f(Ti^{3+}, Ti^{2+})$	$\frac{L \text{ amorphous polymer}}{\text{mol, min}}$	8.0×10^{-2}
C_2 propagation $k_p(Ti^{3+})$	$\frac{L \text{ amorphous polymer}}{\text{mol, mol transition metal, min}}$	8.0×10^{4}
$\frac{k_p(Ti^{2+})}{k_p(Ti^{3+})}$	(—)	1.3
Site Activated by 1-Hexene		
$k_f(Ti^{3+})$	$\frac{L \text{ amorphous polymer}}{\text{mol, min}}$	5.0
C_2 propagation $k_p(Ti^{3+})$	$\frac{L \text{ amorphous polymer}}{\text{mol, mol transition metal, min}}$	5.2×10^{4}

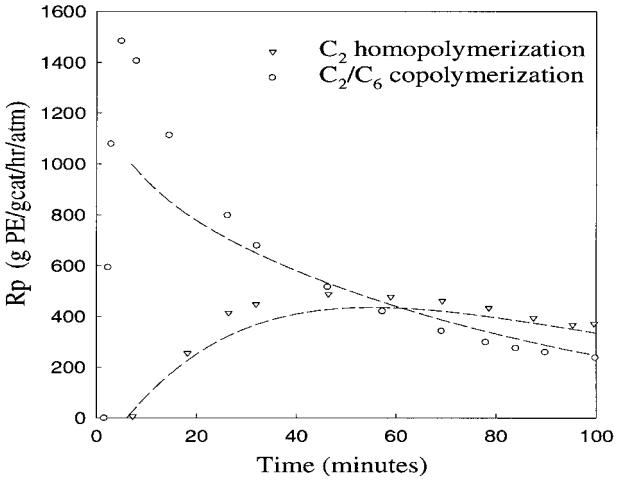

Figure 17 Reaction rates during ethylene homopolymerization and ethylene/hexene copolymerization showing the experimental data[45] and model prediction (lines).

chev[11] examined the dependence of ethylene reaction rate on monomer concentration in a hexane slurry reactor system. It was found that the reaction order changes from about two in ethylene homopolymerization to one in ethylene/hexene copolymerization (Fig. 20). Using the same model parameters as in example 3, this situation is examined. As is shown in Figure 21, our model without parameter fitting predicts a reaction order change from 1.82 for ethylene homopolymerization to 1.14 for ethylene/hexene copolymerization.

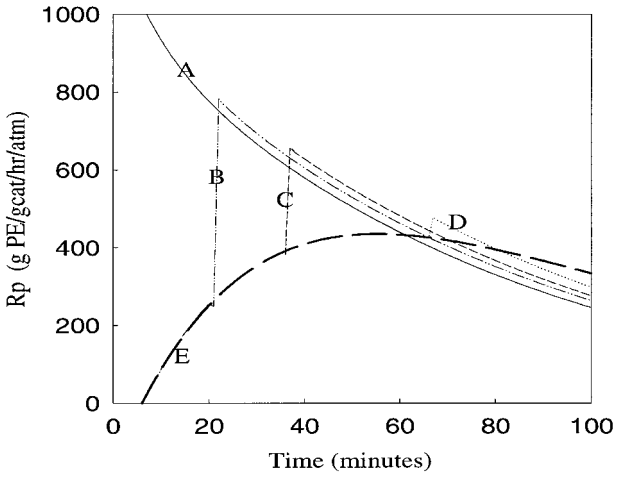

Figure 18 Model simulation examining the effect of delay time of hexene addition on an ongoing ethylene homopolymerization reaction (line E), with delay time of 0 min (A), 15 min (B), 30 min (C), and 60 min (D) (model parameters are listed in Table IV).

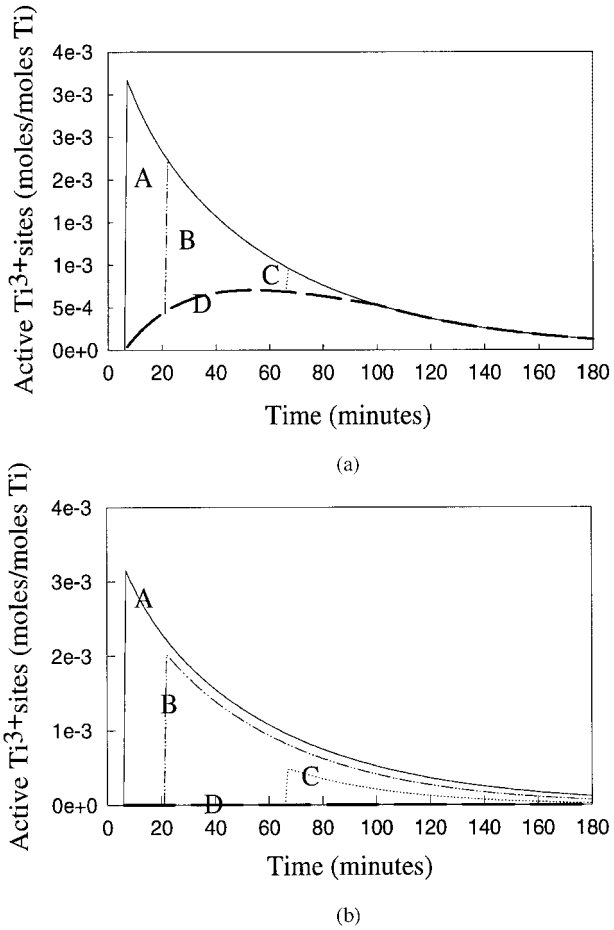

Figure 19 Change of monomer-activated sites during the ethylene polymerization (line D) with delayed hexene addition: delay time of 0 min (A), 15 min (B), and 60 min (C). (a) Total Ti^{3+} sites activated by both ethylene and hexene; (b) Ti^{3+} sites activated by 1-hexene only.

CONCLUSIONS

Using a semi-batch gas phase stirred bed reactor system, ethylene and propylene polymerization experiments were conducted using a magnesium-

supported titanium catalyst. The experimental design was aimed at examining the possible role of the aluminum alkyl in site formation, as well as the participation of monomer in site activation.

In order to capture various well-known kinetic observations in supported titanium catalyzed olefin polymerization, a mathematical model was proposed; the model accounted for both potential site formation by interaction of catalyst and cocatalyst as well as monomer-involved site activation steps. This model was based on two major assumptions: (1) the catalyst activity with respect to different monomers is directly related to the oxidation state of the transition metal, and (2) the differences in kinetic observations between ethylene and other α-olefins is related to their different reaction rate constants in forming active sites.

Using this model together with parameters estimated from various sources, a wide variety of kinetic features previously reported for $MgCl_2$-supported $TiCl_4$/TEA catalyst systems has been successfully predicted. These include the rate enhancement introduced by α-olefins, the effect of Al/Ti ratios on kinetic aspects such as activity and decay rate, and different reaction orders for monomer concentration. This suggests that coupled with suitable parameter estimation schemes, the proposed model and methodology may be used to successfully predict the behavior of a fairly broad class of olefin polymerizations conducted with supported catalysts.

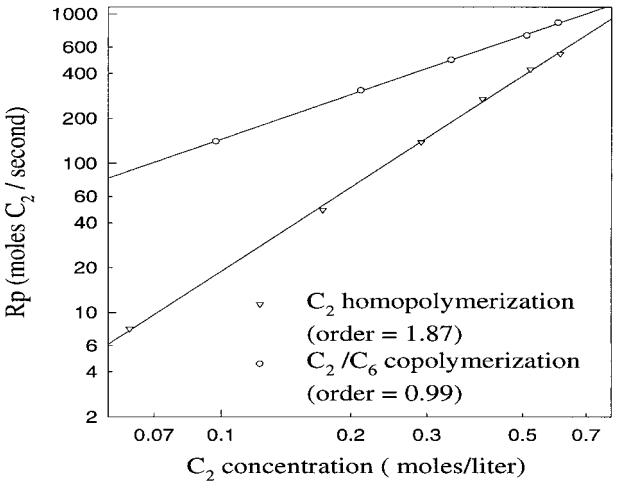

Figure 20 Change of reaction order with respect to ethylene concentration after the addition of hexene: experimental observation from Kryzhanovskii, Gapon, and Ivanchev[11] ($SnCl_4$-modified $TiCl_4/MgCl_2$ catalyst, T = 80°C).

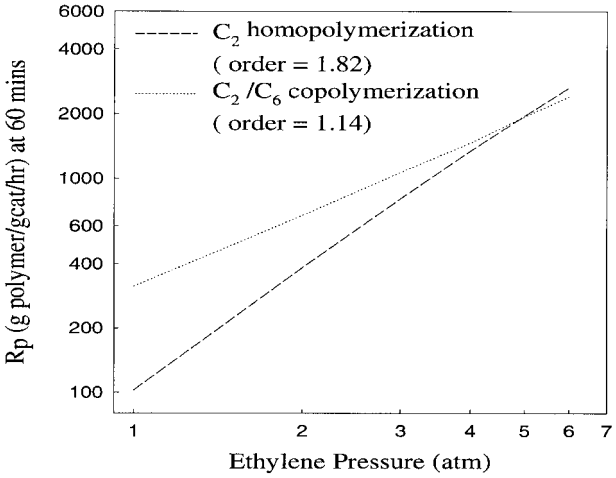

Figure 21 Change of reaction order with respect to ethylene concentration after the addition of hexene: model prediction using same parameters as in example 3.

The authors are indebted to the National Science Foundation and the industrial sponsors of the University of Wisconsin Polymerization Reaction Engineering Laboratory (UWPREL) for support of this research.

REFERENCES

1. P. C. Barbé, G. Cecchin, and L. Noristi, *Adv. Polym.,* **81,** 1 (1986).
2. J. J. A. Dusseault and C. C. Hsu, *J. Appl. Polym. Sci.,* **50,** 431 (1993).
3. F. J. Karol, *Catal. Rev.-Sci. Eng.,* **26,** 557 (1984).
4. V. A. Zakharov, S. I. Makhtarulin, V. A. Poluboyarov, and V. F. Anufrienko, *Makromol. Chem.,* **185,** 1781 (1984).
5. A. A. Baulin, Ye. I. Novikova, G. Ya Mal'kova, V. L. Maksimov, L. I. Vyshinskaya, and S. S. Ivanchev, *Polymer Science U.S.S.R.,* **22,** 205 (1980).
6. C. P. Christenson, J. A. May, and L. E. Freyer, in *Transition Metal Catalyzed Polymerizations, Alkenes, and Dienes,* R. P. Quirk, Ed., Harwood Academic Publishers, New York, 1983, p. 763.
7. P. J. V. Jonnes and R. J. Oldman, in *Transition Metals and Organometallics as Catalysts for Olefin Polymerization,* W. Kaminsky and H. Sinn, Eds., Springer-Verlag, New York, 1988, p. 223.
8. J. C. W. Chien, Siegfried Weber, and Youliang Hu, *J. Polym. Sci., Polym. Chem.,* **27,** 1499 (1989).
9. K. Soga, R. Ohnishi, and T. Sano, *Polymer Bulletin,* **7,** 547 (1982).

10. N. Kashiwa and J. Yoshitake, *Makromol. Chem.,* **185,** 1133 (1984).
11. A. V. Kryzhanovskii, I. I. Gapon, and S. S. Ivanchev, *Kinetics & Catalysis,* **31,** 90 (1990).
12. P. Pino, P. Cioni, J. Wei, B. Rotzinger, and S. Arizzi, *Transition Metals Catalyzed Polymerizations,* R. P. Quirk, Ed., Cambridge University Press, New York, 1988, p. 1.
13. V. Busico, Corradini, A. Ferraro, and A. Proto, *Makromol. Chem.,* **187,** 1125 (1986).
14. C. Dumas and C. C. Hsu, *J. Appl. Polym. Sci.,* **37,** 1605 (1989).
15. C. Dumas and C. C. Hsu, *J. Appl. Polym. Sci.,* **37,** 1625 (1989).
16. U. Giannini, *Makromol. Chem. Suppl.,* **5,** 216 (1981).
17. G. Guastalla and U. Giannini, *Makromol. Chem. Rapid Commun.,* **4,** 519 (1983).
18. T. Keii, E. Suzuki, M. Tamura, M. Murata, and Y. Doi, *Makromol. Chem.,* **183,** 2285 (1982).
19. P. Pino and B. Rotzinger, *Makromol. Chem. Suppl.,* **7,** 41 (1984).
20. L. M. Rimcon-Rubio, C-E. Wilen, and L-E. Lindfors, *Euro. Polym. J.,* **26,** 171 (1990).
21. P. J. T. Tait and Shemin Wang, *Br. Polym. J.,* **20,** 499 (1988).
22. V. Pasquet and R. Spitz, *Makromol. Chem.,* **94,** 451 (1993).
23. F. J. Karol, S-C Kao, and K. J. Cann, *J. Polym. Sci., Polym. Chem.,* **31,** 2541 (1993).
24. Y. V. Kissin, *J. Mol. Catal.,* **56,** 220 (1989).
25. G. C. Han-Adebekun, J. A. Debling, and W. H. Ray, *J. Appl. Polym. Sci.,* submitted.
26. G. C. Han-Adebekun, Ph.D. thesis, Department of Chemical Engineering, University of Wisconsin-Madison, 1996.
27. Bernard Keisch, *The Atomic Fingerprint: Neutron Activation Analysis.* U.S. Atomic Energy Commission, Technical Information Center, New York, 1972.
28. T. R. Crompton, *Analysis of Polymers: an Introduction.* Pergamon Press, New York, 1989.
29. J. J. A. Dusseault and C. C. Hsu, *J. M. S.-Rev. Macromol. Chem. Phys.,* **C33,** 103 (1993).
30. Y. Doi, M. Murata, K. Yano, and T. Keii, *Ind. Eng. Chem. Prod. Res. Dev.,* **21,** 580 (1982).
31. I. Kim, J-H Kim, and S-I Woo, *J. Appl. Polym. Sci.,* **39,** 837 (1990).
32. M. M. V. Marques, Clemente Pedro Nunes, P. J. T. Tait, and Alberto Romao Dias, *J. Polym. Sci., Polym. Chem.,* **31,** 209 (1993).
33. P. C. Barbé, L. Noristi, and M. A. Schexnayder, *Polymerization of Propylene with Magnesium Chloride-Supported Catalysts,* Plenum Press, New York, 1987.
34. C. Beermann and H. Bestian, *Angew. Chem.,* **19,** 618 (1959).
35. A. Malatesta, *Can. J. Chem.,* **37,** 1176 (1959).
36. L. Reich and A. Schindler, in *Polymer Reviews,* H. F. Mark and E. H. Immergut, Eds., Interscience Publishers, New York, 1966, p. 246.
37. H. Bestian and K. Clauss, *Angew. Chem.,* **75,** 1068 (1963).
38. S. A. Sergeev, G. D. Bukatov, V. A. Zakharov, and E. M. Moroz, *Makromol. Chem.,* **184,** 2421 (1984).
39. R. Spitz, L. Duranel, and A. Guyot, *The Mechanism and Stability of Supported Ziegler Catalysts,* Plenum Press, New York, 1987, p. 229.
40. M. L. Cooper and J. B. Rose, *J. Chem. Soc.,* page 795, 1959.
41. R. J. Kern and H. G. Hurst, *J. Polym. Sci.,* **44,** 272 (1960).
42. R. A. Hutchinson and W. H. Ray, *J. Appl. Polym. Sci.,* **41,** 51 (1990).
43. M. Ystenes, *J. Catal.,* **129,** 383 (1991).
44. J. C. W. Chien and C. Kuo, *J. Polym. Sci., Polym. Chem.,* **23,** 761 (1985).
45. D. C. Calabro and F. Y. Lo, in *Transition Metal Catalyzed Polymerization: Ziegler-Natta and Metathesis Polymerization,* R. P. Quirk, Ed., Cambridge University Press, New York, 1988, p. 729.